

Interaction between Earthquake Ground Motion and Multiple Buildings in Urban Regions

Antonio Fernández-Ares,^{a)} and Jacobo Bielak,^{b)}

The main objective of this study is to examine, by means of computational simulation, how earthquake ground motion in an urban region is affected by the presence of multiple building structures, and conversely, how interaction between an individual structure and the surrounding soil and between multiple structures affects structural response during earthquakes. The analysis is based on the Domain Reduction Method (DRM), a modular two-step finite element methodology for modeling earthquake ground motion in highly heterogeneous localized regions. To illustrate the interaction effects, we use an idealized scenario that resembles in a simplified fashion the geological setting of the Mexico City basin and the effects of an earthquake generated some distance away from the basin. A city-like environment, comprised of a set of eighty eight, interacting, 0.5 to 2.0 Hz, simple oscillators with different types of foundations is included in the model. The simplified structures are placed over a soft and dipping clay layer underlain by sands and rock. The results for these scenario earthquakes indicate the occurrence of significant amounts of spatially distributed ground motion, even for relatively small areas of just hundreds of meters. In addition, the dynamic effects generated by the constructed infrastructure alter the way in which seismic waves propagate, and therefore modify the nature of the free field ground motion in and around the vicinity of the urban region. Conversely, the structural response of the individual building models is significantly affected by SSI and structure-to-structure interaction (STSI), resulting in reductions or increases of the response on the order of up to 70 percent with respect to that of the corresponding non-interacting structures. Moreover, same order differences are observed on the response of identical structures that are located at different sites.

INTRODUCTION

Direct observations from earthquake aftershocks have shown that ground motion can vary (by factors of 2 or greater) over 200-m distances for sites on the same geological structure (e.g., Meremonte et al, 1996). Figure 1a shows a map of the San Fernando Valley, Los Angeles basin, and major transportation routes, with the location of the 1994 Northridge mainshock (star), and stations (triangles), and epicenters of aftershocks studied (open circles) by Meremonte et al, 1996 to examine the spatial distribution of ground motion. We focus on the Parking Garage Array located on the Northwest part of the valley, as an area where

^{a)} Paul C. Rizzo Associates, Inc., Monroeville, PA, 15146; antonio.fernandez@rizzoassoc.com

^{b)} Department of Civil and Environmental Engineering, Carnegie Mellon University, Pittsburgh, PA, 15213; jbielak@cmu.edu

damage during the mainshock was strong, and where large spatial variation of the ground motion was observed during aftershocks. Records from various stations within this area are shown in Fig. 1b. These clearly show that the amplitude of the ground motion at station PG1, despite its closeness to stations AB1 and PL1, was several times larger than the motion recorded at the latter stations. PG1 is the location where a parking garage that was severely damaged during the main earthquake stood before the earthquake. The difference in ground motion is partly due to the mechanical properties of the soil in the vicinity of the various stations and to the nature of the ground motion, which at some distance from the epicenter contains significant surface waves. Another factor that may affect the nature of ground motion is the effect that engineering structures might have on the frequency, amplitude, and duration of motion. For instance, Guéguen et al (2000) concluded, using a simplified soil-structure interaction model, that the urban environment did have an important effect on the ground motion in Mexico City during the 1985 earthquake. Wirgin and Bard (1996) performed SSI analysis with simplified models that resemble the Mexico City configuration, and concluded that buildings located in dense urban areas can influence the “free-field” strong motion data, possibly within a 1-km influence radius. Celebi (1995) analyzed data from the Pacific Plaza Building (Emeryville, CA) and its free-field instrumented sites. The instrumented building consists of three symmetric 3-story wings and has two free-field recording stations placed about 30m away from one of its wings. The study concluded that, for this particular building and its recordings, there is pollution of free-field response due to feedback from a nearby structure. A more recent study by Crouse and Ramírez (2003, p. 546, April BSSA) has identified nonlinear site response and kinematic SSI, rather than dynamic SSI, as the main reasons for the differences observed in three sets of building earthquake records at the Jensen Filtration Plant during the 1994 Northridge earthquake mainshock and aftershocks.

In this study we seek to quantify for a particular example, by means of computer modeling, the effect that the presence of an urban environment can have on the free-field ground motion, and the related effect that coupling between multiple structures, their foundations, the soil, and the ground motion have on structural response.

DESCRIPTION OF THE MODEL AND METHODOLOGY

The physical setting for the geological structure is shown in Figure 2. It consists of a shallow basin with a circular plan surrounded by a layered halfspace. The basin is comprised of a soft clay layer over a sand layer, with variable depths, as indicated in Fig. 2b. The thickness of each layer at the center (deepest part) is indicated in the figure. The material properties of the individual soils are also given in the figure. Soil damping is of the Rayleigh type; the maximum fraction of critical damping is on the order of 5% for the softer soils, varies somewhat with frequency, and decreases with the shear wave velocity. The source consists of a double-couple; its location, direction, and slip function are described in Fig. 2c. The analysis is limited to the linear range of behavior.

The building environment is comprised of 88 simple single-story plane structures meant to represent the fundamental mode of more realistic structures. We consider structures with natural periods on the order of 0.5 s, 1.0 s, and 2 s, with 5% of critical damping, and supported on box and/or pile foundations. Details can be found in Fernández-Ares (2003).

We use the DRM, a modular two-step methodology that divides the original problem into two simpler ones (Bielak et al, 2003), to overcome the problem of multiple physical scales that is created by a seismic source that is located at some depth on rock about 10 kilometers

away from the region of interest, and by a region of interest that contains a number of structures distributed over a relatively small area (less than 1 square km) of soft soils within a basin with a 4-km diameter. The first step of the DRM is an auxiliary problem that simulates the earthquake source and propagation path effects with a model that encompasses the source and a background structure from which the localized feature (basin and building structures) have been removed. The second problem models the site effects. Here we use finite elements for both steps. The input is a set of equivalent localized forces derived from the first step. These forces act only within a single layer of elements adjacent to the interface between the exterior region and the geological and building environment features of interest. This enables us to reduce the domain size in the second step. A description on the implementation details and several illustrative examples can be found in Yoshimura et al (2003). In the present application we use the DRM twice. First, to obtain the free field motion within the basin with the structures absent. And then again, to determine the ground motion and structural response within a small portion of the basin with the structures included, using the appropriate seismic excitation.

NUMERICAL RESULTS

In this section we present results of our simulation for the model described above. First we determine the free-field ground motion within the basin due to the double-couple earthquake source, followed by an illustration on how the presence of the structural environment influences the free-field ground motion, and then show how structural response is affected by spatially variable ground motion, SSI, and STSI.

The free-field ground motion within the sedimentary valley is illustrated in Fig. 3. Figure 3a shows the distribution of the amplitude of the peak ground velocity in the EW direction within the basin and its immediate surroundings. This amplitude varies significantly throughout the basin, and exhibits strong edge effects. The detailed seismograms of the EW and NS components of the ground velocity at a particular point near the edge of the basin (shown by an open circle in Fig. 3a) are shown in Fig. 3b, in red. This figure also includes the seismograms that would have been recorded at the same site (in blue), had the valley not been present. Notice the dramatic amplification of ground motion that occurs due to the presence of the valley, and the realistic nature of the seismograms, despite the simple slip function used at the source (Fig. 2a). The corresponding amplitudes of the Fourier transforms of the respective seismograms are also included in Fig. 3. The rich frequency content of this simulated ground motion is noteworthy.

Having determined the free field ground motion, we now place the building structures within a five-block area contained within the dashed region shown in Fig. 3a. As a first case, we consider that only three structures are present within the region of interest, each placed quite far from the other (Structures Nos. 44, 57, and 86 in Fig. 4) in order to minimize the effects of STSI and to assess the effect of the individual structures on the free-field ground motion. As a second example, we populate the entire five-block region with a random arrangement of structures with periods close to 0.5s, 1.0s, and 2.0s, as shown in Fig. 4. Figure 5 shows the spatial distribution of the EW component of peak ground velocity in the EW direction within the region of interest for the three different arrangements: without any structures present; with three isolated 1.0s structures and for the full 5-block “city” with randomly distributed structures. The first observation is that even in the absence of any structures, the ground motion within the 800m x 800m region of interest, exhibits a rapidly varying spatial distribution of ground motion. The three isolated structures have essentially only a local effect on the ground motion, resulting in a considerable reduction of the base

motion at each of the three locations. For the random “city” the ground motion is significantly different from that of the free-field. Important reductions are seen at the building locations; one can almost identify the structures’ footprints. On the other hand, at some locations away from the structures, the amplitude of the polluted ground motion exceeds noticeably that of the free-field.

Finally, Fig. 6 serves to summarize the structural response of the random “city.” Shown in Fig. 6a is the peak interstory drift of the various structures. While some structures exhibit similar peak response, others experience very different response, even for similar natural periods and at nearby locations. To help determine how much of the difference in structural response has to do with differences in the free-field ground motion and how much to structural coupling through the ground, Fig. 6b shows the footprint of the structures superimposed on the distribution of peak ground velocity of the EW component of motion. Thus, for instance, it is possible to see that while the free-field motion at the locations of the structures 83 and 81 is quite similar, the two structures, both with a 1s period, have very different peak response. The same is true for the two 0.5s structures 3 and 6. In these cases the difference of behavior can be attributed to SSI and STSI. On the other hand, structures 21 and 46, both with a natural period of around 1.0s, also exhibit significantly different peak response. Yet, since in this case the free field motion is quite different at the two locations, this difference can be attributed mainly to the difference in ground motion.

CONCLUDING REMARKS

Several conclusion can be drawn from the preceding results: (1) ground motion can vary significantly from one site to another, even within relatively short distances; (2) the constructed facilities within an urban region can significantly pollute the free-field ground motion within that region. Most of the changes in ground motion occur directly beneath the structures; this is due primarily to kinematic interaction. However, also the motion at unoccupied sites can be affected; these changes in the “free-field” motion can either increase or decrease the true free-field response; (3) the structural response is affected strongly by SSI and STSI. Part of the changes are due to kinematic interaction. Inertial interaction, however, also plays an important role.

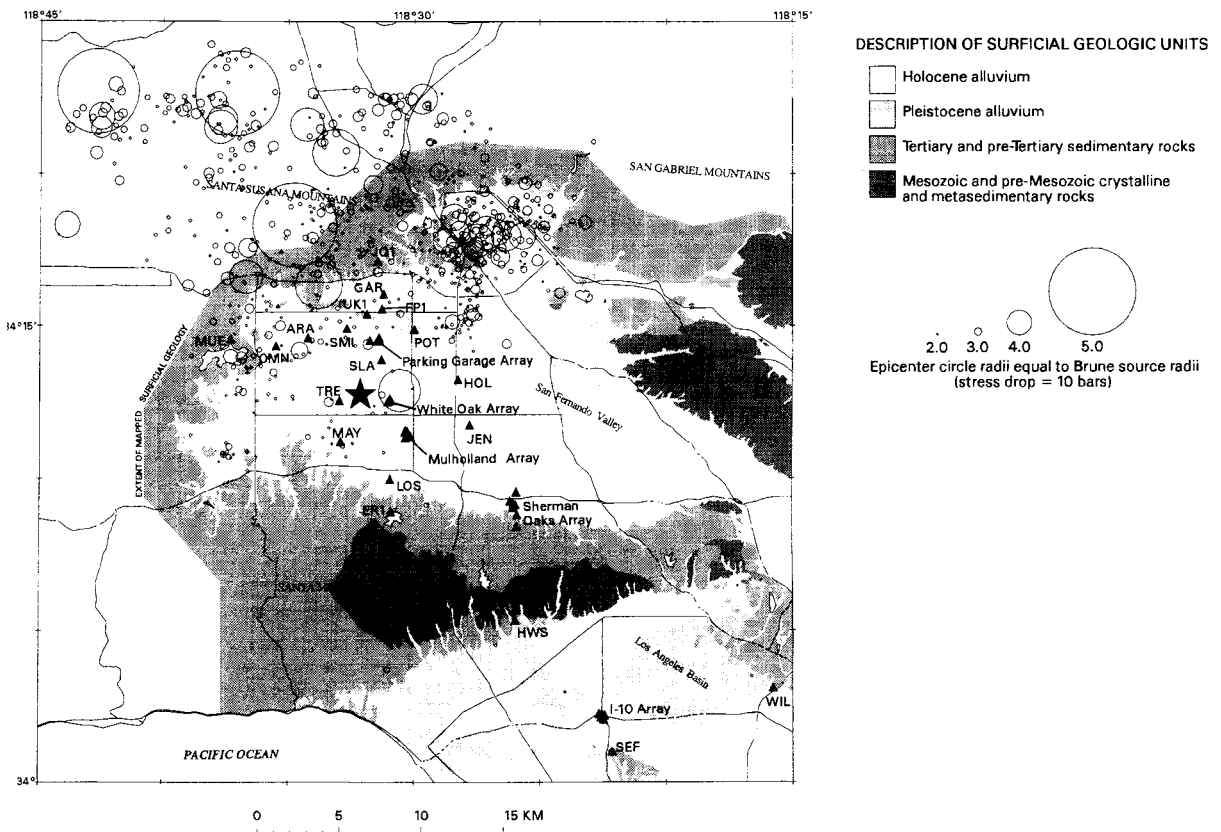
Strictly, these conclusions apply only to the particular soft soils and structure combinations used for this study. However, the qualitative trends in structural behavior are expected to apply also to stiffer soils and structures with similar relative stiffnesses. For the ground motion, the relevant parameter is the wavelength in the soil, i.e., period times shear wave velocity.

ACKNOWLEDGMENT

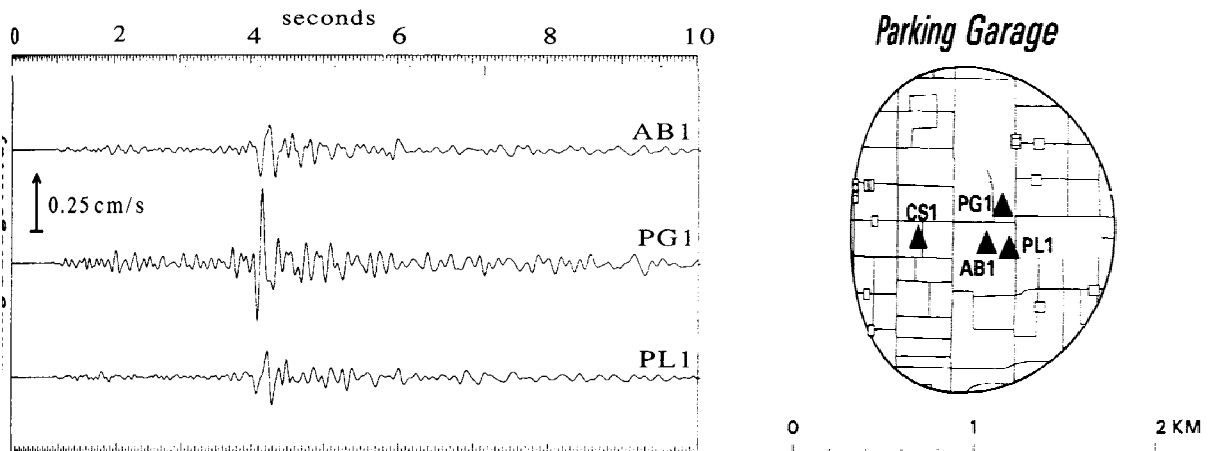
This work was supported by the National Science Foundation, under grants CMS-9980063 of the KDI program, and under grant EEC-0121989 of the Engineering Research Centers. The cognizant program directors were Clifford J. Astill, Joy M. Pauschke, and Aspasia Zerva. We are grateful for this support.

REFERENCES

- Bielak, J., Loukakis, K., Hisada, Y., and Yoshimura, C., 2003. Domain reduction method for three-dimensional earthquake modeling in localized regions, Part I: Theory, *Bull. Seism. Soc. Am.*, **93** (2), 817-824.
- Celebi, M., 1995. *Free-field motions near buildings*, Proc. 10th European Conf. on Earthq. Eng., 215-221.
- Crouse, C. B. and Ramirez, J. C., 2003. Soil-structure interaction and site response at the Jensen Filtration Plant during the 1994 Northridge, California Mainshock and Aftershocks, *Bull. Seism. Soc. Am.*, **93** (2), 546-556.
- Fernández-Ares, A., 2003. *Urban seismology: interaction between earthquake ground motion and response of urban regions*. Ph.D. Thesis. Carnegie Mellon University, Pittsburgh, PA, 15213.
- Guéguen, P., Bard, P. Y., and Semblat, J. F., 2002. *Engineering seismology: seismic hazard and risk analysis: seismic hazard analysis from soil-structure interaction to site-city interaction*. Proc. 12th World Conf. on Earthq. Eng., Auckland, NZ.
- Meremonte, M., Frankel, A., Cranswick, E., Carver, D., and Worley, D., 1996. Urban seismology-Northridge aftershocks recorded by multi-scale arrays of portable digital seismographs, *Bull. Seism. Soc. Am.*, **86** (5), 1350-1363.
- Wirgin, A. and Bard, P. Y., 1996. Effects of buildings on the duration and amplitude of ground motion in Mexico City, *Bull. Seism. Soc. Am.*, **86** (3), 9140920.
- Yoshimura, C., Bielak, J., Hisada, Y., and Fernández, A., 2003. Domain reduction method for three-dimensional earthquake modeling in localized regions, Part II: Verification and Applications, *Bull. Seism. Soc. Am.*, **93** (2), 825-840.

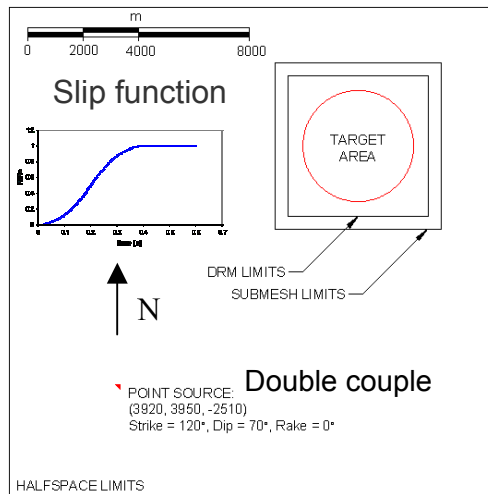


(a)



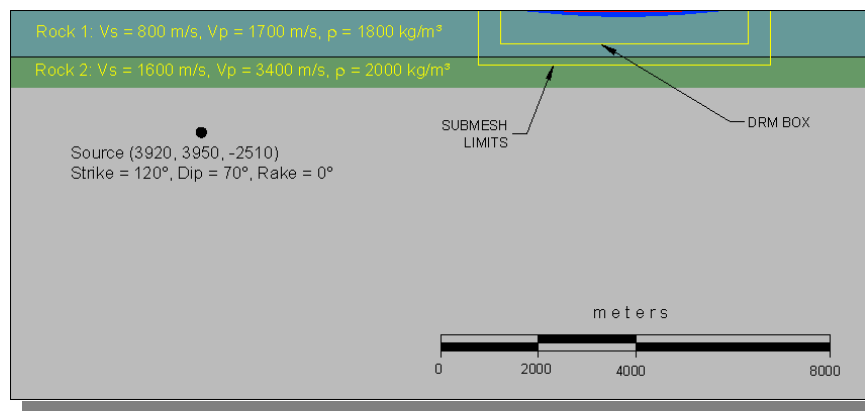
(b)

Figure 1. (a) Map of the San Fernando Valley, Los Angeles Basin, major transportation routes, epicenters, and stations. The Parking Garage Array is in the NW quadrant of the valley; (b) Record of an 1994 Northridge earthquake aftershock showing NS component of velocity at various stations. (After Meremonte et al, 1996).

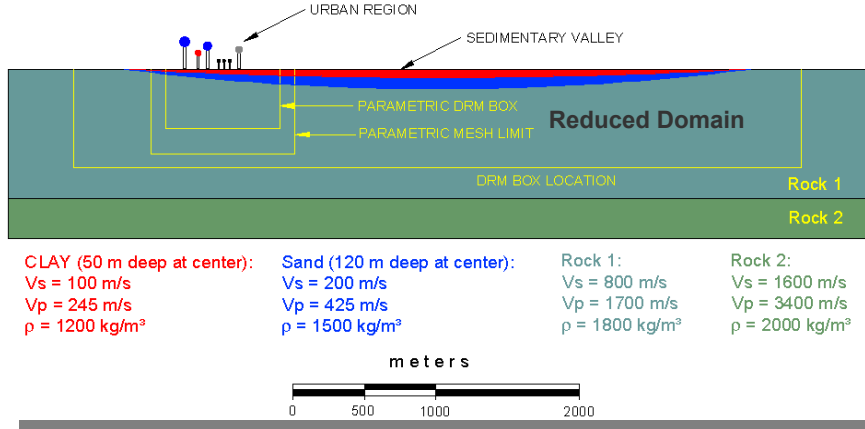


(a)

Cross Section



(b)



(c)

Figure 2. Model basin and background geological structure. (a) Plan view and seismic source location, direction, and slip function; (b) Vertical cross section in EW direction of entire geological structure; (c) Vertical cross section in EW direction of region of interest encompassing the valley (showing the urban region), and surrounding layered structure

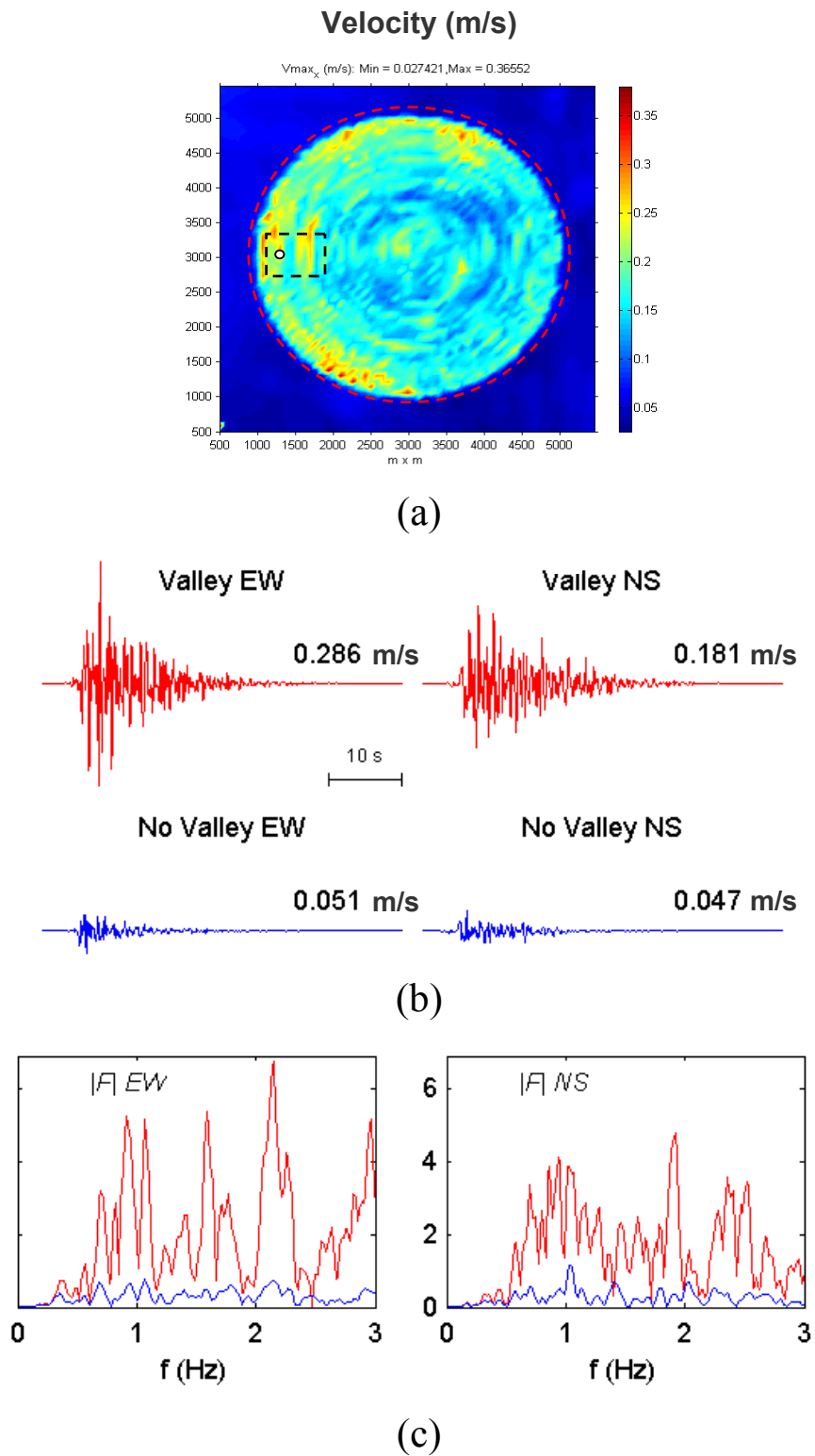


Figure 3. Free-field surface velocity within the basin and its immediate vicinity. (a) maximum velocity distribution in EW direction; (b) synthetic velocity seismograms at location (a) indicated by open circle, with and without the valley present; (c) amplitudes of the corresponding Fourier transforms.

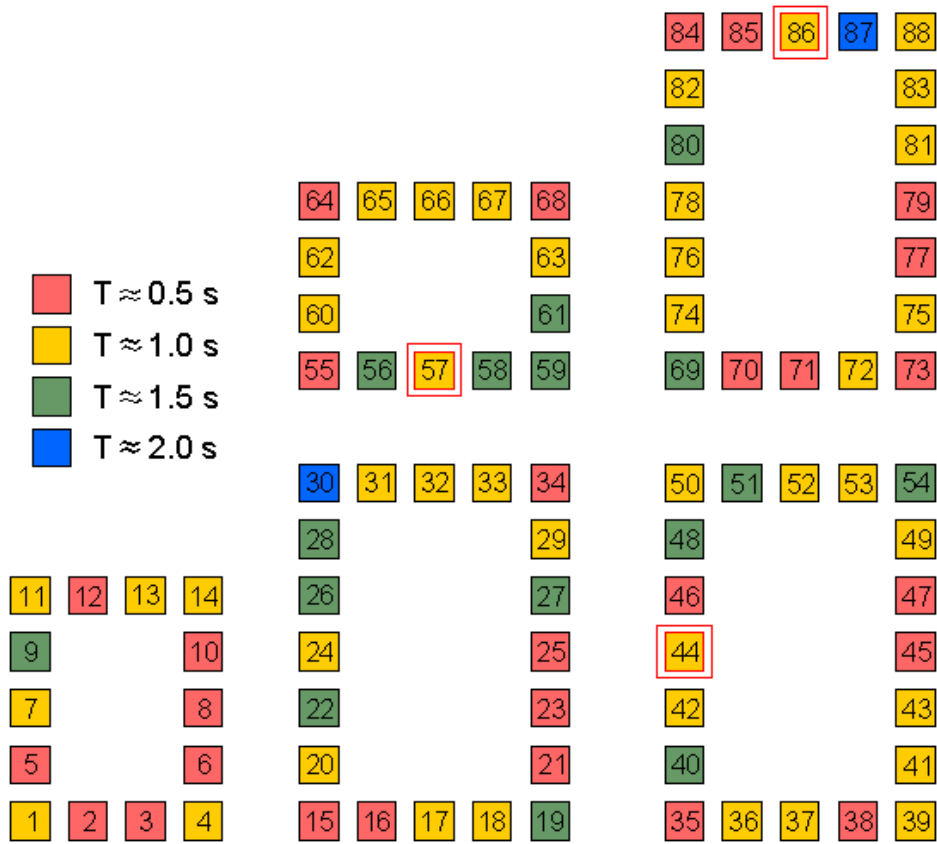
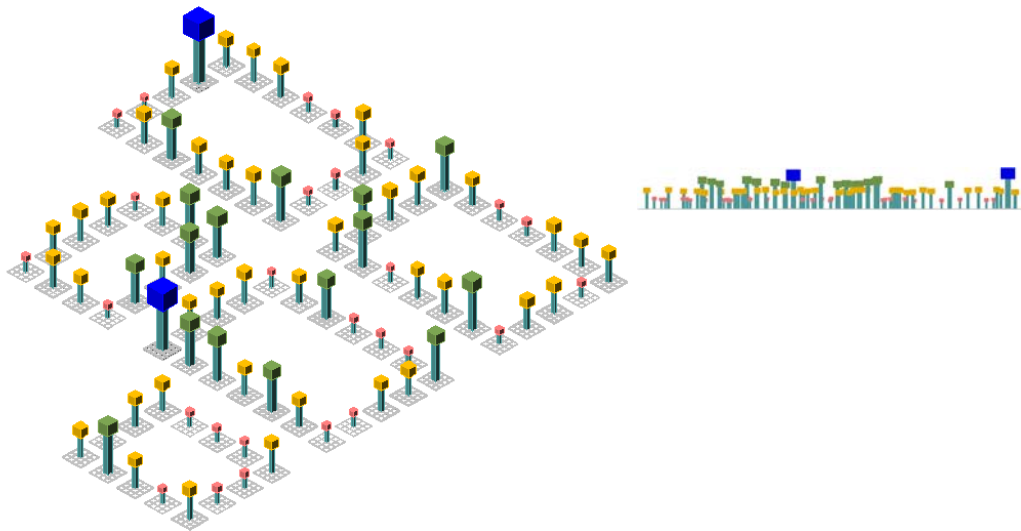
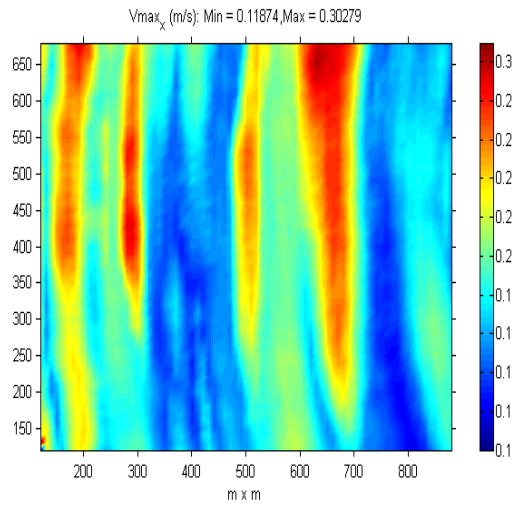
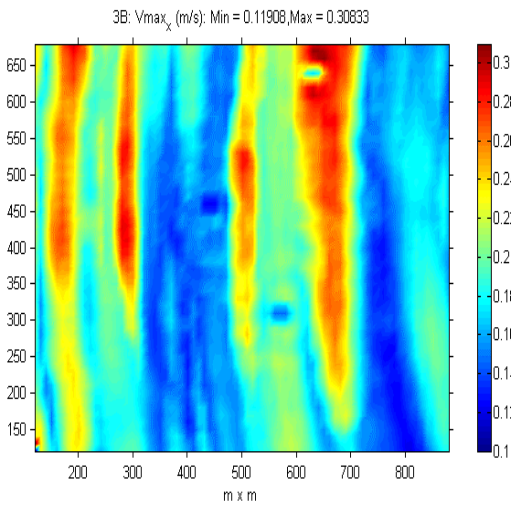


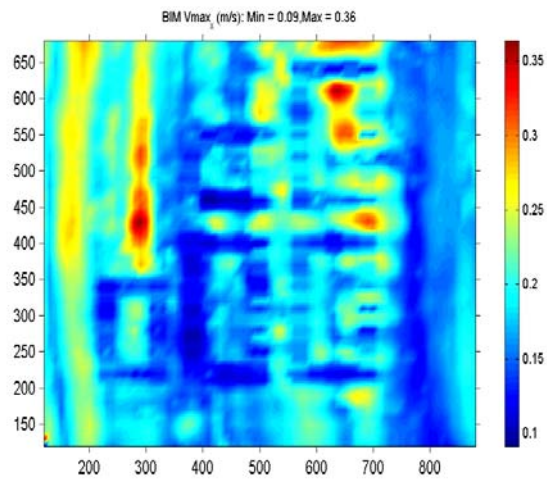
Figure 4. Random “city” with numbered structures. Colors and height of structures indicate their natural periods.



Free-Field

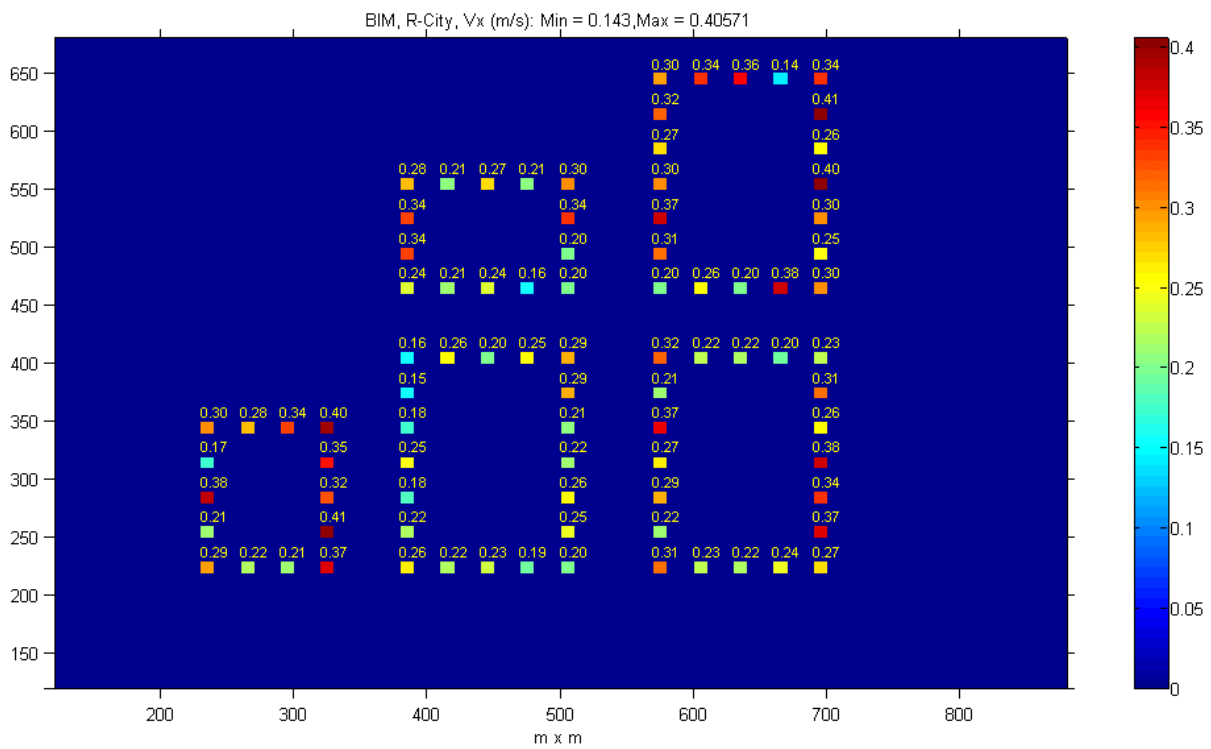


Three 1.0-sec Buildings

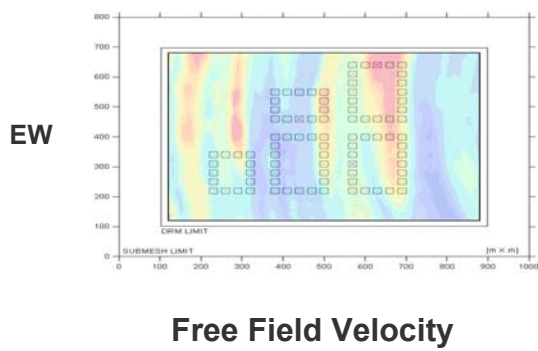


Random City

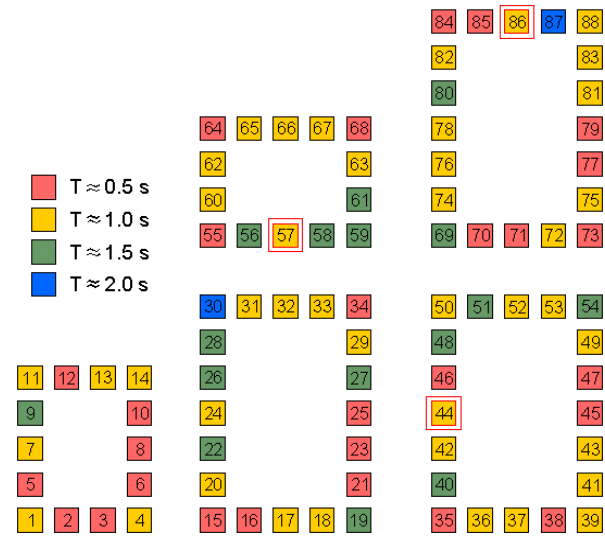
Figure 5. Distribution of peak ground velocities in EW direction for three different environments



(a)



(b)



(c)

Figure 6. (a) Peak interstory velocity (in m/s) in EW direction of the random “city” structures; (b) Peak free-field velocity distribution with structures’ layout superimposed; (c) Numbered structures; color denotes natural period.